

# Synthesis and Application of Carbon–Iron Oxide Microspheres’ Black Pigments in Electrophoretic Displays

Xianwei Meng · Ting Wen · Shiwei Sun ·  
Rongbo Zheng · Jun Ren · Fangqiong Tang

Received: 21 June 2010/Accepted: 1 July 2010/Published online: 15 July 2010  
© The Author(s) 2010. This article is published with open access at Springerlink.com

**Abstract** Carbon–iron oxide microspheres’ black pigments (CIOMBs) had been prepared via ultrasonic spray pyrolysis of aqueous solutions containing ferrous chloride and glucose. Due to the presence of carbon, CIOMBs not only exhibited remarkably acid resistance, but also could be well dispersed in both polar solvents and nonpolar solvent. Finally, dispersions of hollow CIOMBs in tetrachloroethylene had successfully been applied in electrophoretic displays.

**Keywords** E-paper · Pigment · Black · Carbon

## Introduction

Electrophoretic displays (EPDs) have been the subject of intense research and development for a number of years [1–5]. In such displays, pigments are dispersed as a colloidal suspension in a colored solvent, which is placed in a narrow space between two transparent electrodes. By applying an electric field to the suspension, the charged pigments can be moved through the fluid. When the field is applied in one direction, the pigments move toward the observer and the pixel has the color of the pigments. When the field is applied in the opposite direction, the ITO electrode closest to the observer is covered with colored solvent. Just like printed paper, EPDs are lightweight, flexible and easy to read in all lighting conditions [6–9].

Above of all, they provide an important improvement in the field of power consumption: due to the bistability of the pigments, an image is retained on the display without the need for constant refreshment. Their properties make them the most likely candidate in the search for a display that combines the benefits of printed paper and an image display. EPDs are now used in consumer products such as the Amazon Kindle or Sony E-Reader. Nevertheless, problems with the long-term image quality of the displays have prevented their widespread usage. For example, pigments that make up EPDs tend to settle, resulting in inadequate service life for the displays [10–13].

The change in the appearance of a pixel of the EPDs is solely due to the change of the position of the pigments within the suspension. Thus, the pigments play a vital role on the speed and efficiency of the EPDs. For a white/black display cell, the white particles are typically titanium oxide because of its relatively high refractive index of 2.7, which leads to excellent scattering properties [14]. Generally, carbon black is the material of choice to produce the black color in most applications. However, carbon black has a complex and poorly understood surface chemistry, which may vary widely with the specific raw material and the exact process used for the carbon black production. Furthermore, carbon black has a poorly understood aggregate, fractal structure. It has also been discovered that carbon black has a low density ( $0.8 \text{ g/cm}^3$ ), which is not matched to that of the usual suspending medium (about  $1.7 \text{ g/cm}^3$ ) [15]. There is thus a need for black particle with proper density and surface chemistry for used in EPDs that can be compatible with the suspending fluid.

Herein, we demonstrate that carbon–iron oxide microspheres’ black pigments (CIOMBs) are formed via ultrasonic spray pyrolysis of the aqueous solutions containing  $\text{FeCl}_2$  and glucose. Different from the formation process of

X. Meng · T. Wen · S. Sun · R. Zheng · J. Ren · F. Tang (✉)  
Laboratory of Controllable Preparation and Application of  
Nanomaterials, Technical Institute of Physics and Chemistry,  
Chinese Academy of Sciences, 100190 Beijing, People’s  
Republic of China  
e-mail: tangfq@mail.ipc.ac.cn

carbon powders, in situ-formed iron oxide nanoparticles are introduced as surface chemistry and density modification component to form carbon–iron oxide composites. The density of the CIOMBs can be easily tuned in the range of 1.5–2.2 g/cm<sup>3</sup> by acid etching, which resolved the problem of mismatched density between carbon-based black pigment and electrophoretic medium. The CIOMBs can be well dispersed in various solvents including polar solvents (water, methanol, ethanol, etc.) and nonpolar solvent (e.g. tetrachloroethylene) due to their surfaces are functionalized with abundant functional groups such as OH, COH and CH<sub>2</sub>. The CIOMBs can be used as effective black electrophoretic particle for electrophoretic displays.

## Experimental

Ferrous chloride (FeCl<sub>2</sub>), glucose, and HCl solution (12 M), titania, DISERBYK-161 were purchased and used without further purification. Deionized water was used throughout this work.

The USP experimental setup is similar to that of Suslick's group [16–19]. In a typical experiment, 0.5 mol/L glucose and 0.8 mol/L FeCl<sub>2</sub> were added to deionized water so as to form a precursor solution under magnetic stirring. For nebulization, a Yuyue household ultrasonic humidifier was used to nebulize a precursor solution into a fine mist. The furnace temperature was set as 700°C with a nitrogen flow rate of 2 SLPM (Standard Liters per Minute). After 1 h of collection into water-filled beaker, the black product was collected with a magnet. After washed with deionized water and then ethanol three more times, the black sample was collected for further analysis.

In order to tune the density of CIOMBs, as-prepared CIOMBs were immersed in concentrated HCl (12 M) at room temperature for 1–12 h. The content of iron oxide in the composite dissolve in the concentrated HCl gradually, which leads to decrease in the CIOMBs' density. Furthermore, CIOMBs were washed with deionized water and then ethanol three more times, and the black sample was collected for further analysis.

Electrophoretic dispersions were prepared via dispersing of CIOMBs (0.05 g/mL) and titania (0.10 g/mL) in tetrachloroethylene using DISERBYK-161 (0.01 g/mL) as a dispersant. It is then introduced in an electrophoretic cell, composed of two ITO-coated glasses (3.0 × 7.0 cm) sealed with 75 μm thickness, and the electrode area was prepared by a photoetching technique. The cell is operated using a Keithley 230 programmable power source.

X-ray diffraction (XRD) patterns were obtained on Rigaku Dmax2000 with Cu K $\alpha$  radiation. The morphology of the samples was examined by scanning (SEM, XL30ESEM FEG) and transmission (TEM, JEOL 2010)

electron microscopy. Fourier transform infrared spectrum (FT-IR) of the samples was recorded at the ambient temperature on a Nicolet 560 Fourier Transform Infrared Spectrometer with the resolution factor of ±0.1 cm<sup>-1</sup>.

## Results and Discussions

In the present route, ultrasound is used to produce aerosol droplets dispersed in nitrogen via ultrasonic spray treatment of precursor aqueous solution. The aerosol droplets are carried in nitrogen stream through a quartz-glass tube in a hot furnace, and water evaporation and precursor decomposition occur, generating CIOMBs. With USP, the aerosol droplets will act as individual micrometer-sized chemical reactors to impose morphology control on the target products.

Herein, ferrous chloride and glucose are used as precursor of iron oxide and carbon, respectively, to form CIOMBs via USP. The morphology of the product is studied by both scanning electron microscopy (SEM) and transmission electron microscopy (TEM). The overall morphology of CIOMBs is revealed in Fig. 1, which indicates that the sample is composed of a large quantity of core–shell microspheres with the size in the range of 1–3 μm. From Fig. 1, we can see that the initial concentration of FeCl<sub>2</sub> has influence on both the size and the morphology of CIOMBs. As shown in Fig. 1a, the size of CIOMBs is in the range of 300–1,400 nm when the concentration of FeCl<sub>2</sub> is 0.08 M. The surface of as-prepared spheres is smooth. When the concentration of FeCl<sub>2</sub> is 0.32 M, the size of sample will increase to 500–3,000 nm. In addition, the surface becomes rough, which comprises iron oxide nanoparticles with size of about 50–100 nm (the inset of Fig. 1b). Furthermore, microspheres with Fe-rich core/C-rich shell (the size is in the range 500–3,000 nm) are formed when the concentration of FeCl<sub>2</sub> reaches up to 0.8 M. As shown in Fig. 1c, d, as-prepared spheres display two distinct surfaces: bubble-like surface and rough surface. That is, some spheres have bubble-like carbon surface (consists of many bubble in the carbon surface), and Fe-rich core comprises the agglomeration of iron oxide nanoparticles. The other spheres have rough carbon-rich shell (the thickness is about 100 nm) and Fe-rich core (Fig. 1d and the inset of Fig. 1c).

The possible formation mechanism of CIOMBs can be illustrated as follows: (1) Carbonaceous nanoparticles loaded with Fe<sup>2+</sup>/Fe<sup>3+</sup> ion are generated via the catalyzing of Fe<sup>2+</sup> [20, 21]; (2) With the furnace temperature increasing, carbon-coated iron oxide nanoparticles will be formed via the oxidization of iron ion, accompanying by the further carbonization of carbonaceous components with the catalysis of in situ-formed iron oxide [21]; (3) With the

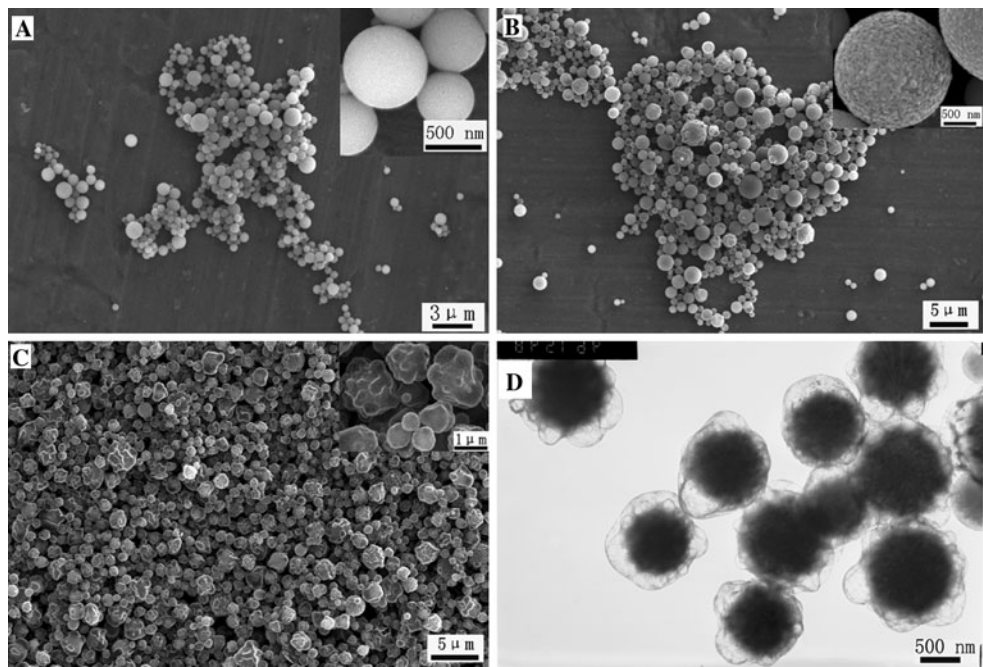


**Fig. 1** SEM and TEM images of core/shell CMM obtained via USP of glucose and  $\text{FeCl}_2$  with different initial concentration of  $\text{FeCl}_2$ : **a** 0.08 M; **b** 0.32 M; **c, d** 0.8 M. The inset of **a–c** is the high-magnification SEM images of corresponding samples

reaction time prolonging, more carbon will be formed in the neighborhood of aforementioned iron oxide nanoparticles via the carbonization of glucose. When the initial concentration of  $\text{FeCl}_2$  is low, as-produced CIOMBs display smooth surface, in which iron oxide nanoparticles are randomly dispersed in the carbon spheres (Fig. 1a). When the initial concentration of  $\text{FeCl}_2$  is high enough, as-produced CIOMBs display rough surface due to aforementioned iron oxide nanoparticles tend to agglomerate to form iron oxide-rich core (Fig. 1b–d). With the reaction time prolonging, subsequently generated carbon will be formed carbon shell around the iron oxide-rich core.

Figure 2 shows the XRD pattern of aforementioned CIOMBs. As shown in Fig. 2, the diffraction peaks can be indexed to the mixture of face-centered cubic  $\text{Fe}_3\text{O}_4$  (JCPDS file No. 48-1487) and hexagonal-structured  $\alpha\text{-Fe}_2\text{O}_3$  (JCPDS file No.33-0664). There are no obvious crystalline peaks of carbon, indicating that the structure of carbon is amorphous.

The FT-IR spectrum is used to identify the surface chemistry present in the CIOMBs. Overall, in the range of 1,000–3,500  $\text{cm}^{-1}$ , the spectrum is similar to that of carbon spheres obtained via the hydrothermal treatment of glucose aqueous solution [22]. As shown in Fig. 3, the bands at 3,400 and 1,625  $\text{cm}^{-1}$  can be assigned to the O–H and C=C, respectively. The bands in the range 1,000–1,400  $\text{cm}^{-1}$  can be attributed to C–OH stretching vibration and O–H bending vibrations. It should be noted that the bands at 2,925 and 2,855  $\text{cm}^{-1}$ , which can be

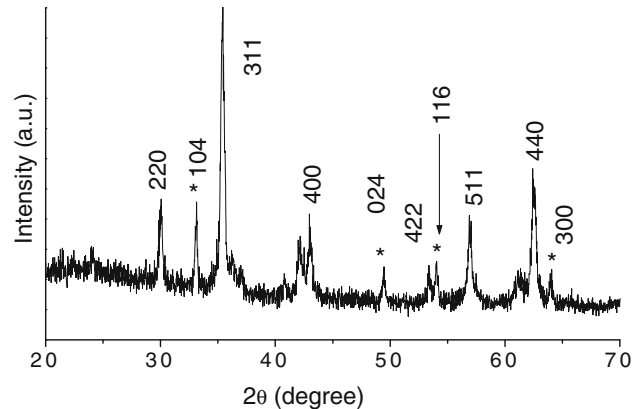


**Fig. 2** XRD patterns of CIOMBs prepared. Notes: The peaks labeled by \* can be indexed to  $\alpha\text{-Fe}_2\text{O}_3$  (JCPDS file No. 33-0664)

assigned to hydrogen bonded sp<sup>3</sup> carbon [23], are stronger than those of the pure carbon sphere, while the band at 1,710 (C=O) is almost disappear. The reason may lie on the relative higher reaction temperature (700 vs. 180°C), which leads to the more complete carbonization of glucose. In the case of three bands (455, 535 and 570  $\text{cm}^{-1}$ ) in the range of 500–700  $\text{cm}^{-1}$ , they can be assigned to  $\text{Fe}_3\text{O}_4$  and  $\text{Fe}_2\text{O}_3$ , respectively. Both  $\text{Fe}_3\text{O}_4$  and  $\text{Fe}_2\text{O}_3$  exist in the spectrum of sample CIOMBs, which are consistent with the results of XRD (Fig. 3).

As demonstrated in the previous literatures, both crude carbon blacks and crude carbon nanotubes are hard dispersed in either polar or nonpolar solvents. In the case of

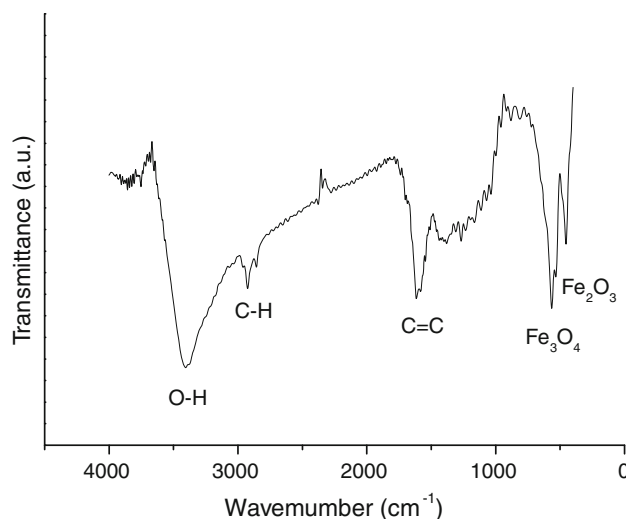


**Fig. 3** FT-IR spectra of sample CIOMBs

carbon spheres obtained via the dehydration of polysaccharides aqueous solution under hydrothermal conditions (<200°C), they exhibit excellent dispersibility in polar solvents including water and ethanol. However, they are also hard to disperse in nonpolar solvent such as tetrachloroethylene. The dispersibility of CIOMBs is investigated via dispersing CIOMBs in various solvents. Poor dispersion usually limits their application in EPDs. It is well known that surface's functional groups play important roles in the process of dispersion. As shown in Fig. 3, there are abundant functional groups (OH, COH, CH<sub>2</sub>, etc.) on the surface of CIOMBs, which lead to good dispersibility in various solvents. The CIOMBs not only can be dispersed in polar solvents (i.e. water, methanol and ethanol), but also can be dispersed in nonpolar solvent, such as tetrachloroethylene. The proved surface chemistry makes CIOMB a versatile black pigment for EPDs.

The density of the as-prepared CIOMBs is about 2.2 g/cm<sup>3</sup>, which makes CIOMBs gravitational settling in tetrachloroethylene (density, 1.63 g/cm<sup>3</sup>) due to the density mismatch (Fig. 4a). In order to decrease the density,



**Fig. 5** Photograph of Black–White electrophoretic display cell

CIOMBs are dipped in the concentrated HCl (12 M). The iron oxide nanoparticles instead of carbon in the composite can react with HCl, and the product can dissolve in the solution. Thus, the density of CIOMBs decreases during the HCl etching. When the duration of etching is 1 h, the CIOMBs can be well dispersed in tetrachloroethylene, whose density is about 1.7 g/cm<sup>3</sup>, which is a good density match. When the duration of etching is 12 h, the density of CIOMBs is too light to be dispersed in tetrachloroethylene. Most of the CIOMBs float on the surface of the suspension. From the TEM pictures, the decrease in iron oxide content in the composite can be distinguished.

Exploiting their well dispersibility in tetrachloroethylene, CIOMBs are used as black electrophoretic particles for electrophoretic displays. Electrophoretic dispersions are prepared via dispersing of sample CIOMBs and titania (served as white electrophoretic particles) in tetrachloroethylene using DISERBYK-161 as a dispersant. After above dispersions are introduced into an electrophoretic cell, an electrophoretic display is formed. Fig. 5 presents photographs of an electrophoretic display with dimensions of 75 μm (*t*) × 7 cm (*w*) × 3 cm (*l*) after applying 30 V.

## Conclusions

In summary, using aqueous solutions containing ferrous chloride and glucose as precursors, a simple and

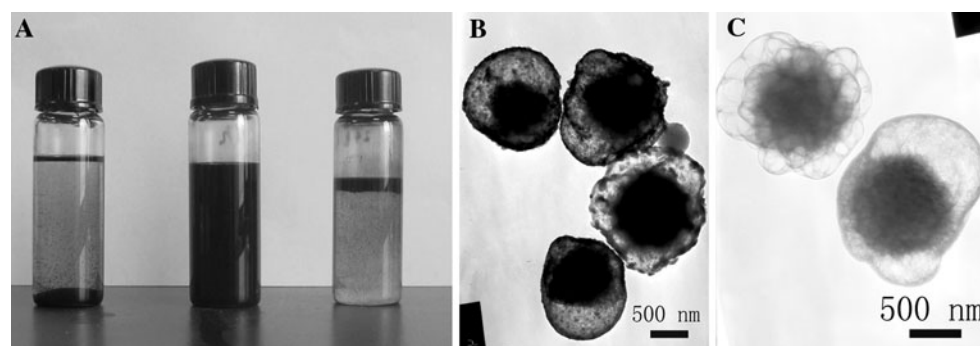


**Fig. 4** **a** CIOMBs with different etching time (from left to right 0, 1, 12 h) are dispersed in tetrachloroethylene. TEM images of CIOMBs with 1 h (**b**) and 12 h etching

continuous strategy is developed to synthesize CIOMBs via USP. Due to the presence of affluent functional groups in their surface, CIOMBs can be dispersed in water, methanol, ethanol and tetrachloroethylene. By adjusting the concentrated HCl etching duration, the density of CIOMBs can be tuned to match that of tetrachloroethylene. The surface chemistry and density of as-prepared CIOMBs are appropriate for EPDs assembly. An EPD is formed using CIOMBs as black electrophoretic particles in tetrachloroethylene.

**Acknowledgments** This work was financially supported by the National Hi-Tech 863 Programme (2009AA03Z302), National Science Foundation of China (60736001, 60907042), and Beijing Natural Science Foundation (2093044).

**Open Access** This article is distributed under the terms of the Creative Commons Attribution Noncommercial License which permits any noncommercial use, distribution, and reproduction in any medium, provided the original author(s) and source are credited.

## References

1. B. Comiskey, J.D. Albert, Y. Hidekazu, J. Joseph, *Nature* **394**, 253 (1998)
2. R.A. Hayes, B.J. Feenstra, *Nature* **425**, 383 (2003)
3. A.C. Arsenault, D.P. Puzzo, I. Manners, G.A. Ozin, *Nat. Photonics* **1**, 468 (2007)
4. D.P. Puzzo, A.C. Arsenault, I. Manners, G.A. Ozin, *Angew. Chem. Int. Ed.* **47**, 1 (2008)
5. D.G. Yu, J.H. An, J.Y. Bae, S.D. Ahn, S.Y. Kang, K.S. Suh, *Macromolecules* **38**, 7485 (2005)
6. J.P. Wang, X.P. Zhao, H.L. Guo, *Opt. Mater.* **30**, 1268 (2008)
7. Y.T. Wang, X.P. Zhao, D.W. Wang, *J. Microencapsul.* **23**, 762 (2006)
8. Y. Chen, X. Wang, R.C. Liang, *US Pat.* 7564614B2 (2009)
9. H.S. Kang, H.J. Cha, J.C. Kim, *Mol. Cryst. Liq. Cryst.* **472**, 247 (2007)
10. C.H. Honeyman, E.A. Moran, L. Zhang, A.E. Pullen, E.J. Pratt, K.L. Houde, M.A. King, C.A. Herb, R.J. Paolini, *US Pat.* 6822782B2 (2004)
11. A.E. Pullen, T.H. Whitesides, C.H. Honeyman, B. Comiskey, J.D. Albert, *US Pat.* 7002728B2 (2006)
12. X.W. Meng, F.Q. Tang, B. Peng, J. Ren, *Nanoscale Res. Lett.* **5**, 174 (2010)
13. M.P.L. Werts, C. Brochon, G. Hadzioannou, *Chem. Mater.* **20**, 1292 (2008)
14. B. Peng, F.Q. Tang, D. Chen, X.L. Ren, X.W. Meng, J. Ren, *J. Colloid Interface Sci.* **329**, 62 (2009)
15. A.E. Pullen, T.H. Whitesides, C.H. Honeyman, B. Comiskey, J.D. Albert, *US Pat.* 7247379B2 (2007)
16. Y.T. Didenko, K.S. Suslick, *J. Am. Chem. Soc.* **127**, 12196 (2005)
17. S.E. Skrabalak, K.S. Suslick, *J. Am. Chem. Soc.* **128**, 12642 (2006)
18. S.E. Skrabalak, K.S. Suslick, *J. Phys. Chem. C* **111**, 17807 (2007)
19. J.H. Bang, K. Han, S.E. Skrabalak, H. Kim, K.S. Suslick, *J. Phys. Chem. C* **111**, 10959 (2007)
20. X.J. Cui, M. Antonietti, S.H. Yu, *Small* **2**, 756 (2006)
21. M.M. Titirici, M. Antonietti, A. Thomas, *Chem. Mater.* **18**, 3808 (2006)
22. X.M. Sun, Y.D. Li, *Angew. Chem. Int. Ed.* **43**, 597 (2004)
23. F.Y. Cao, C.L. Chen, Q. Wang, Q.W. Chen, *Carbon* **45**, 727 (2007)